

# Synthesis and Characterization of a Saddle-Shaped Nickel–Carbene Complex Derived from an Imidazolium-Linked *meta*-Cyclophane

Murray V. Baker,<sup>\*,1</sup> Brian W. Skelton, Allan H. White, and Charlotte C. Williams

Department of Chemistry, The University of Western Australia, Crawley, WA 6009, Australia

Received December 4, 2001

A novel nickel complex in which the nickel center is bonded to two pyridine units and two heterocyclic carbene units in an imidazolium linked *meta*-cyclophane skeleton has been synthesized and structurally characterized. Both the parent imidazolium-linked cyclophane and the nickel complex undergo H/D exchange reactions in D<sub>2</sub>O solutions.

## Introduction

Inspired by recent interest in transition metal complexes of imidazolium “Arduengo-type” carbenes,<sup>2</sup> we have explored the chemistry of a variety of imidazolium-linked cyclophanes<sup>3</sup> and the synthesis of some palladium and nickel complexes of heterocyclic carbenes derived from imidazolium-linked *ortho*-cyclophanes.<sup>4</sup> Palladium–carbene complexes in which the heterocyclic carbene units are incorporated into a rigid *ortho*-cyclophane skeleton are exceptionally active catalysts for Heck and Suzuki couplings,<sup>4</sup> and these palladium complexes are significantly more stable than related complexes in which the heterocyclic carbenes are part of less rigid ligand frameworks.<sup>5</sup> Imidazolium-linked *meta*-cyclophanes have also been reported<sup>6</sup> and have shown anion-binding properties in solution.<sup>7</sup> A palladium complex of an imidazolium-linked *meta*-cyclophane has been reported to have good activity as a Heck catalyst, but the structure of that catalyst is uncertain.<sup>8</sup>

In the cyclophane-based nickel– and palladium–carbene complexes referred to above, the cyclophane skeleton consists of benzene rings linked by imidazolium units, so the only strongly coordinating groups in the cyclophane skeleton are the heterocyclic carbene units. There are, however, a variety of functionalized imidazolium salts (noncyclophane) that have been converted into polydentate ligands that bind to metal centers via both a heterocyclic carbene and a weaker donor (e.g., pyridine).<sup>8–12</sup> Garrison et al. have described the synthesis and characterization of a pyridine-based imida-

zolium-linked *meta*-cyclophane, **1**, which contains pyridine units as potential coordinating groups. A dimeric silver–carbene complex derived from **1** was reported, but in that complex the pyridine units were not directly bonded to a metal center.<sup>13</sup> Here we report our own work with **1** and its conversion into a novel nickel complex, **2**, in which the nickel center is bonded to both the pyridine units and the heterocyclic carbene units of the cyclophane skeleton.

## Results and Discussion

**Synthesis and NMR Behavior of the Cyclophane.** Cyclophane **1** was prepared by addition of an acetone solution of 2,6-bis(bromomethyl)pyridine to an acetone solution of 2,6-bis(imidazol-1-ylmethyl)pyridine and stirring the reaction mixture at room temperature for several days, yielding the cyclophane as a white precipitate of high purity. A lower yielding, but faster, method involves the addition of equal amounts of the bis(bromomethyl)pyridine and bis(imidazolylmethyl)pyridine to a smaller volume of either acetone or acetonitrile and refluxing overnight. Although the product obtained from both methods is usually pure enough for use in further reactions, analytically pure samples may be readily obtained by recrystallization from methanol.

The <sup>1</sup>H NMR spectra of the cyclophane **1** in DMSO-*d*<sub>6</sub> and methanol-*d*<sub>4</sub> solutions at ambient temperature show the expected resonances, including a singlet for the benzylic protons, consistent with the macrocyclic ring being conformationally labile on the NMR time scale. Imidazolium-linked *ortho*-cyclophanes show some conformational mobility that can be frozen out at low

(1) To whom correspondence should be addressed. Fax: +61 8 9380 1005. E-mail: mvb@chem.uwa.edu.au.

(2) Arduengo, A. J., III; Harlow, R. L.; Kline, M. *J. Am. Chem. Soc.* **1991**, *113*, 361–363.

(3) Baker, M. V.; Bosnich, M. J.; Williams, C. C.; Skelton, B. W.; White, A. H. *Aust. J. Chem.* **1999**, *52*, 823–825.

(4) Baker, M. V.; Skelton, B. W.; White, A. H.; Williams, C. C. *J. Chem. Soc., Dalton Trans.* **2001**, 111–120.

(5) Herrmann, W. A.; Elison, M.; Fischer, J.; Köcher, C.; Artus, G. R. *J. Angew. Chem., Int. Ed. Engl.* **1995**, *34*, 2371–2373.

(6) Alcalde, E.; Ramos, S.; Pérez-García, L. *Org. Lett.* **1999**, *1*, 1035–1038.

(7) Alcalde, E.; Alvarez-Rúa, C.; García-Rodríguez, S.; Mesquida, N.; Pérez-García, L. *J. Chem. Soc., Chem. Commun.* **1999**, 295–296.

(8) Magill, A. M.; McGuinness, D. S.; Cavell, K. J.; Britovsek, G. J. P.; Gibson, V. C.; White, A. J. P.; Williams, D. J.; White, A. H.; Skelton, B. W. *J. Organomet. Chem.* **2001**, *617–618*, 546–560.

(9) McGuinness, D. S.; Cavell, K. J. *Organometallics* **2000**, *19*, 741–748.

(10) Tulloch, A. A. D.; Danopoulos, A. A.; Kleinhenz, S.; Light, M. E.; Hursthouse, M. B.; Eastham, G. *Organometallics* **2001**, *20*, 2027–2031.

(11) Peris, E.; Loch, J. A.; Mata, J.; Crabtree, R. H. *J. Chem. Soc., Chem. Commun.* **2001**, 201–202.

(12) Gründemann, S.; Albrecht, M.; Loch, J. A.; Faller, J. W.; Crabtree, R. H. *Organometallics* **2001**, *20*, 5485–5488.

(13) Garrison, J. C.; Simons, R. S.; Talley, J. M.; Wesdemiotis, C.; Tessier, C. A.; Youngs, W. J. *Organometallics* **2001**, *20*, 1276–1278.

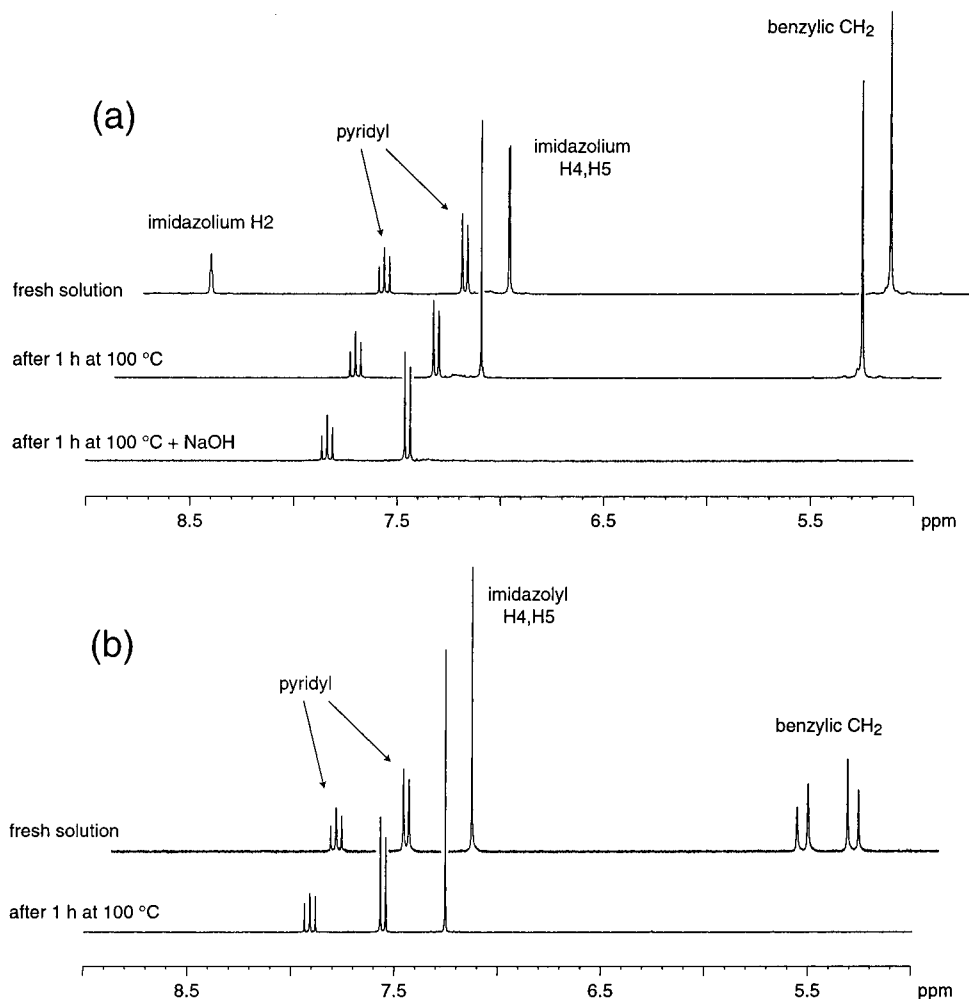
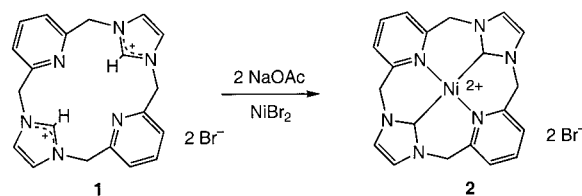


**Figure 1.**  $^1\text{H}$  NMR spectra (300 MHz,  $\text{D}_2\text{O}$ ) for solutions of (a) the cyclophane salt **1** and (b) the nickel complex **2**, before and after H/D exchange.

temperatures,<sup>4</sup> but the spectra of methanol- $d_4$  solutions of **1** did not change when the temperature was lowered to  $-53$  °C.

The cyclophane **1** shows interesting H/D exchange reactions in  $\text{D}_2\text{O}$  solutions (Figure 1a). The imidazolium H2 protons ( $\delta$  8.67) exchange rapidly with deuterium from the solvent, so much so that even at room temperature the  $^1\text{H}$  NMR signal for the H2 protons always “underintegrates” in spectra recorded from  $\text{D}_2\text{O}$  solutions. When a fresh solution of **1** in  $\text{D}_2\text{O}$  is heated for 1 h at 100 °C (steam bath), the H2 protons are fully exchanged, as indicated by disappearance of the H2 signal from the  $^1\text{H}$  NMR spectrum. Addition of 2 equiv of NaOH to the sample and a further 1 h of heating at 100 °C caused the imidazolium H4/H5 protons ( $\delta$  7.23) as well as the benzylic protons ( $\delta$  5.38) to also undergo complete exchange with deuterium from the solvent, so that only the signals due to the pyridyl aromatic protons remained in the  $^1\text{H}$  NMR spectrum. The ability of imidazoles and imidazolium ions to undergo H/D exchange at C2 and C4/5 is well known,<sup>14–17</sup> while exchange at the benzylic positions is likely a consequence of the enhancement of acidity of these positions by the pyridine group.<sup>18</sup>

#### Scheme 1



**Nickel Complexation Studies.** Treatment of **1** with  $\text{NiBr}_2$  and NaOAc in DMSO at 85 °C for 72 h readily afforded the nickel compound **2** (Scheme 1) as a yellow powder in 52% yield. The product is diamagnetic and air-stable and was conveniently recrystallized from hot water. The compound is probably best described as a bromide salt of the cation  $[\text{NiL}]^{2+}$  (L = the bis(carbene) obtained by removal of the two imidazolium H2 protons from **1**), with L coordinating to the nickel center via two pyridine nitrogens and two heterocyclic carbenes. The  $^{13}\text{C}$  NMR spectrum of **2** showed a resonance due to the carbene carbons at  $\delta$  165.3 ( $\text{D}_2\text{O}$  solution), whereas in the spectrum of **1** the imidazolium C2 carbons resonated

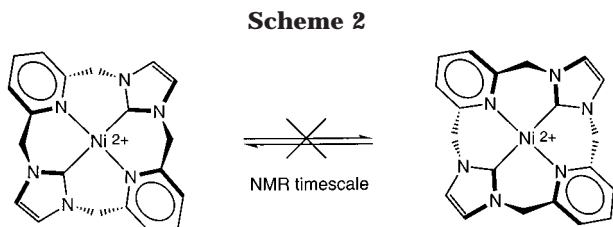
(14) Wong, J. L.; Keck, J. H., Jr. *J. Org. Chem.* **1974**, *39*, 2398–2403.

(15) Takeuchi, Y.; Yeh, H. J. C.; Kirk, K. L.; Cohen, L. A. *J. Org. Chem.* **1978**, *43*, 3565–3570.

(16) Hardacre, C.; Holbrey, J. D.; McMath, S. E. *J. Chem. Soc., Chem. Commun.* **2001**, 367–368.

(17) Denk, M. K.; Rodezno, J. M. *J. Organomet. Chem.* **2001**, 617–618, 737–740.

(18) Abu-Shanab, F. A.; Wakefield, B. J.; Elnagdi, M. H. *Adv. Heterocycl. Chem.* **1997**, *68*, 181–221.



at  $\delta$  153.6 ( $D_2O$  solution). The  $^1H$  NMR spectrum of **2** (Figure 1b) shows an AB pattern for the benzylic protons, indicative of a restriction of conformational mobility for the cyclophane skeleton upon complexation. The simplicity of the  $^1H$  and  $^{13}C$  NMR spectra is consistent with the macrocycle in  $[NiL]^{2+}$  adopting a puckered conformation (cf. the crystal structure, below) with  $C_2$  axes defined by the carbene carbons and the pyridine nitrogens. A ring twisting process that would interconvert two enantiomeric conformations can be envisaged (Scheme 2), and this process would interconvert the chemically nonequivalent benzylic protons. The puckered conformation, however, is rigid on the NMR time scale; no broadening of the benzylic AB pattern was detected even at 80 °C (300 MHz  $^1H$  NMR,  $D_2O$  solution).  $^1H$  NMR spectra recorded from  $D_2O$  solutions at elevated temperatures revealed the onset of an H/D exchange process. The benzylic protons in  $[NiL]^{2+}$  were fully exchanged within 1 h at 100 °C (Figure 1b), but there was no evidence for H/D exchange of pyridyl or imidazolyl protons even after the sample was heated at 100 °C overnight.

Addition of small quantities of  $Ag^+$  (as a solution of  $AgNO_3$  in  $D_2O$ ) to  $D_2O$  solutions containing **2** and 1,3,5-trioxane (internal integration standard) resulted in formation of a cream-colored, light-sensitive precipitate (presumably  $AgBr$ ). Precipitation was complete when ca. 2 equiv of  $Ag^+$  had been added. During this experiment, there was no change in the  $^1H$  NMR spectrum of the sample. This result is consistent with our formulation of the complex as  $[NiL]^{2+}$  rather than  $[NiLBr]^+$  or  $[NiLBr_2]$  and is not surprising given the long  $Ni\cdots Br$  distances in the solid-state structure (see below).

**Structural Comment.** Crystals adequate for the X-ray work were grown by slow evaporation of an aqueous solution of the complex. The stoichiometry and connectivity observed are consistent with the formulation  $2 \cdot 3H_2O$ , one formula unit, devoid of crystallographic symmetry, comprising the asymmetric unit of the structure. Residues modeled as water molecule oxygen atoms (O(1)) or fragments thereof (O(2–5), some dispositions too close for simultaneous occupancy) lie in a tunnel through the structure about the crystallographic  $a$  axis. Associated disorder may or may not be concerted with that of the complex, which may or may not be regarded as ionic. The nickel atom lies in a quasi-planar four-coordinate array with *trans* pairs of nitrogen atoms and carbene carbons, disposed in two moieties differing in site occupancy. The major moiety is shown in Figure 2a, site occupancy 0.797(1); a minor moiety, modeled with complementary occupancy, inhabits a similar space, but is rotated by ca. 90°, so that its five-membered carbenoid rings lie approximately in the location of the pyridine rings of the major component, closely for major rings 1,3, more divergent for rings 2,4 (Table 1, Figure 2b). A view of the two systems in

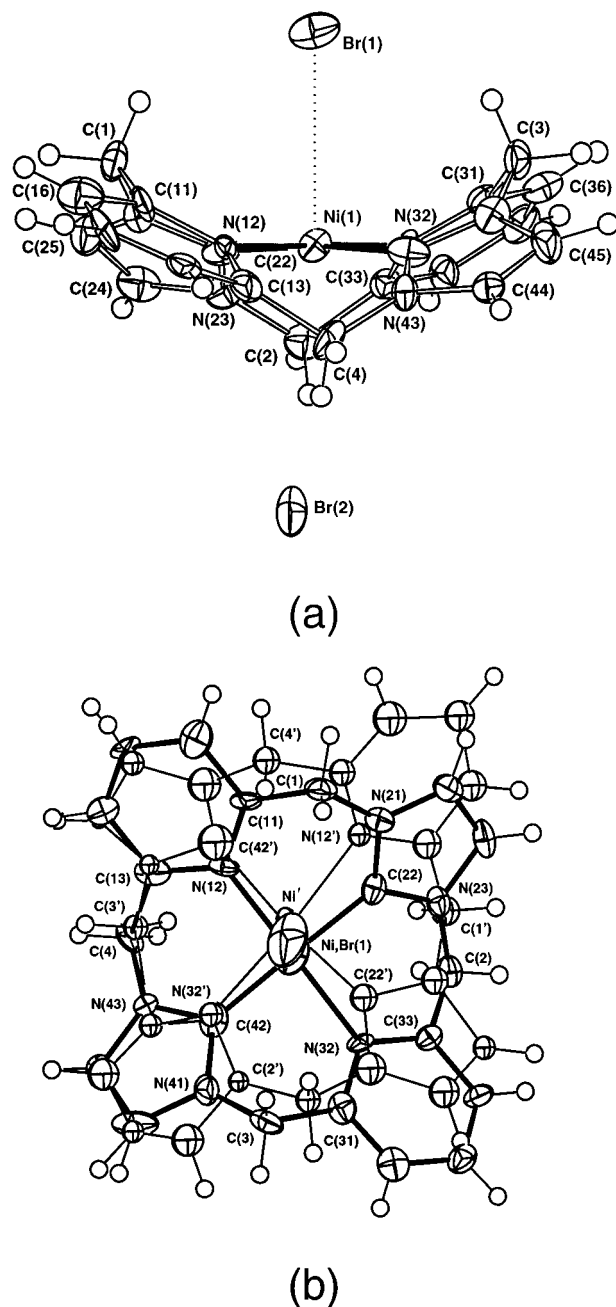


**Figure 2.** (a) Side-on view of the major component of **2**, showing  $[NiL]^{2+}$  in association with the pair of bromide ions. 50% probability amplitude displacement ellipsoids are shown for the non-hydrogen atoms, hydrogen atoms having arbitrary radii of 0.1 Å. (b) Projection of the pair of ligand components about the  $Br-Ni$  line, bonds of the non-hydrogen atom moiety of the major component being shown as solids.

superposition is given in Figure 2b. The nickel atom is modeled similarly as disposed over a pair of sites separated by 0.479(5) Å. The bromide counterions approach the nickel atom from either side of the four-coordinate plane, offering incipient six-coordination. The  $Ni\cdots Br$  distances are long and different, however, with the disorder of the  $NiL$  system mimicked by disorder in the two bromide ions,  $Br(1)\cdots Br(1')$  0.270(7),  $Br(2)\cdots Br(2')$  0.391(5) Å, with possible further ramifications extending into the solvent system as noted above. (We conduct discussion hereafter in terms of the more



**Table 1.** Selected Molecular Core Geometries for 2 (Major (Unprimed) Component)<sup>a</sup>

atoms	parameter	atoms	parameter
Distances (Å)			
Ni–N(12)	1.981(6)	Ni–C(22)	1.870(8)
Ni–N(32)	2.003(6)	Ni–C(42)	1.834(9)
Ni···Br(1)	3.146(1)	Ni···Br(2)	3.928(1)
Angles (deg)			
N(12)–Ni–C(22)	90.1(3)	N(32)–Ni–C(22)	90.3(3)
N(12)–Ni–C(42)	91.3(3)	N(32)–Ni–C(42)	88.2(4)
N(12)–Ni–N(32)	179.2(3)	C(22)–Ni–C(42)	174.3(4)
Ni–N(12)–C(11)	118.9(5)	Ni–N(32)–C(31)	121.3(5)
Ni–N(12)–C(13)	121.4(5)	Ni–N(32)–C(33)	120.4(5)
Ni–C(22)–C(21)	127.5(6)	Ni–C(42)–C(41)	129.3(7)
Ni–C(22)–N(12)	126.7(6)	Ni–C(42)–C(43)	125.3(7)
N(12)–C(11)–C(1)	123.9(7)	N(32)–C(31)–C(3)	122.9(8)
N(12)–C(13)–C(4)	121.3(7)	N(32)–C(33)–C(2)	121.0(7)
C(22)–N(21)–C(1)	120.5(7)	C(42)–N(41)–C(3)	120.3(7)
C(22)–N(23)–C(2)	120.3(7)	C(42)–N(43)–C(4)	124.0(7)
C(11)–C(1)–N(21)	112.3(7)	N(23)–C(2)–C(33)	109.8(7)
C(31)–C(3)–N(41)	112.6(7)	N(43)–C(4)–C(13)	110.3(7)

<sup>a</sup> For the minor component, Ni···Br(1', 2') are 3.242(7), 3.878(5); Ni···Ni' is 0.479(5), Br(1)···Br(1') 0.270(7), Br(2)···Br(2') 0.391(5); C(1)···C(4') is 1.11(3), C(2)···C(1') 1.08(4), C(3)···C(2') 0.86(3), C(4)···C(3') 0.25(3), N(12)···C(42') 0.50(4), C(22)···N(12') 1.00(3), N(32)···C(22') 0.81(3), C(42)···N(32') 0.12(3) Å. Dihedral angles between the N<sub>2</sub>C<sub>2</sub> coordination plane and ring planes 1–4 are 28.9(3)°, 32.6(3)°, 32.6(3)°, 31.4(3)° (unprimed), 30(1)°, 30(1)°, 31(1)°, 34(1)° (primed component), and between superimposed pairs 1/4', 2/3', 3/2', 4/3' 5.5(8)°, 60.3(9)°, 3.2(9)°, 64.5(9)°.

precisely described major component of the array, the minor aggregate exhibiting little substantive difference (Table 1.) Ni···Br(1) at 3.146(1) Å is shorter than Ni···Br(2) (3.928(1) Å), the bonding status of both interactions being dubious. Contacts between the Br atoms and neighboring methylene hydrogen atoms differ in concert, those at C(1,3) contacting Br(1) at 2.7<sub>9</sub>, 2.8<sub>2</sub> Å, with those at C(2,4) contacting Br(2) more unsymmetrically (2.8<sub>8</sub>, 3.0<sub>4</sub> Å). The inclinations of the pyridyl and imidazolyl rings relative to the central N<sub>2</sub>C<sub>2</sub> plane ( $\chi^2$  62;  $\delta$ Ni 0.039(1) Å) are similar, dihedrals being 28.9–(3)°, 32.6(3)° (rings 1,3) and 32.6(3)°, 31.4(3)° (rings 2,4), spread over a wide range, and generating an overall “saddle” array in which the component planes are intersected by the median N<sub>2</sub>C<sub>2</sub> plane, the total array being of C<sub>2</sub> symmetry. The bridging methylene groups alternately deviate to either side of the N<sub>2</sub>C<sub>2</sub> plane (Figure 2a) in contrast to, for example, some nickel complexes of “saddle” porphyrins<sup>19</sup> in which the methylene groups are coplanar with the central N<sub>4</sub> plane while the pyrrolyl planes deviate alternately to either side. While rather variable, perhaps in response to “lattice forces”, e.g., N–Ni–N is 179.2(3)°, but C–Ni–C 174.3(4)°, the exocyclic angular geometries to the component rings are essentially “normal” and not suggestive of any considerable strain in the macrocycle, such as exists presumably being absorbed in the conformational warp of the “saddle”. Nevertheless, Ni–C(22,42) are 1.870(8), 1.834(9) Å, rather shorter than in the (*trans*) Ni–C distances found in (e.g.) the bis(chelate)Ni complex of Douthwaite et al.<sup>20</sup> (1.936(4), 1.928(4) Å), but closely similar to the value of 1.862(2) Å reported recently.<sup>4</sup>

(19) Mandon, D.; Ochsenein, P.; Fischer, J.; Weiss, R.; Jayaraj, K.; Austin, R. N.; Gold, A.; White, P. S.; Brigaud, O.; Battioni, P.; Mansuy, D. *Inorg. Chem.* **1992**, *31*, 2044–2049.

## Experimental Section

**General Considerations.** Nuclear magnetic resonance spectra were recorded on Bruker AM 300 (300.1 MHz for <sup>1</sup>H, 75.5 MHz for <sup>13</sup>C) or ARX 500 (500.13 MHz for <sup>1</sup>H, 125.8 MHz for <sup>13</sup>C) spectrometers at ambient temperature. Chemical shifts are referenced with respect to solvent signals. Assignments of <sup>13</sup>C NMR spectra were made with the aid of DEPT and <sup>1</sup>H–<sup>13</sup>C HMQC spectra. Mass spectra (FAB) were recorded using a VG Autospec mass spectrometer with a cesium ion source and a *m*-nitrobenzyl alcohol matrix. Microanalyses were performed by the Microanalytical Laboratory at the Australian National University, Canberra. All solvents were redistilled (under the laboratory atmosphere) prior to use, except for *N,N*-dimethylformamide (APS Finechem, AR grade), which was used as received, and dimethyl sulfoxide (Ajax Chemicals, AR grade), which was dried over 4 Å molecular sieves.

**2,6-Bis(1H-imidazol-1-ylmethyl)pyridine.** A solution of imidazole (1.28 g, 19 mmol) and powdered KOH (1.17 g, 21 mmol) in DMF (40 mL) was stirred for 30 min. 2,6-Bis-(bromomethyl)pyridine<sup>21</sup> (2.5 g, 9.4 mmol) was added portionwise, and the pale yellow suspension was stirred at room temperature overnight. The solvent was removed under vacuum, the oily residue was suspended in refluxing CHCl<sub>3</sub> (65 mL) for 10 h, and the resulting off-white solid resulted from the rather sticky residue. This precipitate was recrystallized from methanol to remove impurities (1.74 g, 77%). Spectroscopic properties were as expected.<sup>22</sup>

**Cyclophane Salt (1).** A solution of 2,6-bis(bromomethyl)pyridine (110.7 mg, 0.418 mmol) in acetone (50 mL) was added dropwise with stirring to a solution of 2,6-bis(1H-imidazol-1-ylmethyl)pyridine (100.0 mg, 0.418 mmol) also in acetone (50 mL). This mixture was stirred at room temperature for several days, during which time the cyclophane precipitated as a white powder (150 mg, 71%). The powder was used without further purification for complexation reactions, while an analytically pure sample was obtained by recrystallization from methanol. (Found: C, 45.89; H, 4.46; N, 15.55. C<sub>20</sub>H<sub>20</sub>N<sub>6</sub>Br<sub>2</sub>·1.25H<sub>2</sub>O requires C, 45.60; H, 4.31; N, 15.95). Spectroscopic properties match those reported.<sup>13</sup>

**Cyclophane–Nickel Complex (2).** A mixture of **1** (150.8 mg, 0.299 mmol) and NaOAc (56.4 mg, 0.688 mmol) was dissolved in a minimum amount of DMSO (3–4 mL) in a Schlenk flask fitted with a Young's tap. The solvent was removed in vacuo at 60 °C, and the flask was back-filled with nitrogen. Under a nitrogen atmosphere, anhydrous NiBr<sub>2</sub> (71.9 mg, 0.329 mmol) and more dry DMSO (8 mL) were added, the flask was sealed, and the mixture was heated to 85 °C for 3 days. A yellow-orange precipitate formed. The mixture was allowed to cool to room temperature, and the supernatant was drawn off by a pipet. Removal of residual DMSO in vacuo at ca. 60 °C left the cyclophane complex **2** as an orange powder (88 mg, 52%), which was spectroscopically pure. Samples for microanalysis and X-ray studies were recrystallized from water. (Found: C, 38.74; H, 3.57; N, 13.42. C<sub>20</sub>H<sub>18</sub>N<sub>6</sub>NiBr<sub>2</sub>·3H<sub>2</sub>O requires C, 39.06; H, 3.93; N, 13.67). <sup>1</sup>H NMR (500.13 MHz, D<sub>2</sub>O):  $\delta$  7.95 (t, *J* = 7.8 Hz, 2H, 2 × pyridyl-H4); 7.61 (d, *J* = 7.8 Hz, 4H, 4 × pyridyl-H3/H5); 7.30 (s, 4H, 4 × imidazolium H4/H5); 5.70 (d, *J* = 15.9 Hz, 4H, 4 × CHH); 5.45 (d, *J* = 15.9 Hz, 4H, 4 × CHH). <sup>13</sup>C NMR (125.8 MHz, D<sub>2</sub>O + acetone):  $\delta$  54.4 (CH<sub>2</sub>); 122.0 (CH, imidazolium C4/C5); 127.1 (CH, pyridyl-C3/C5); 141.8 (CH, pyridyl-C4); 157.2 (C, pyridyl-C2/C6); 165.3 (Ni–C). Mass spectrum: *m/z* 481.013572 [C<sub>20</sub>H<sub>18</sub>N<sub>6</sub>Ni<sup>81</sup>Br (NiL<sup>81</sup>Br<sup>+</sup>) requires 481.010932]; 479.012787 [C<sub>20</sub>H<sub>18</sub>N<sub>6</sub>Ni<sup>79</sup>Br (NiL<sup>79</sup>Br<sup>+</sup>) requires 479.012978].

(20) Douthwaite, R. E.; Haüssinger, D.; Green, M. L. H.; Silcock, P. J.; Gomes, P. T.; Martins, A. M.; Danopoulos, A. A. *Organometallics* **1999**, *18*, 4584–4590.

(21) Baker, W.; Buggle, K. M.; McOmie, J. F. W.; Watkins, D. A. M. *J. Chem. Soc.* **1958**, 3594–3603.

(22) Herrmann, W. A.; Köcher, C.; Goossen, L. J. US Patent 6 025 496, CAN 127:318962.

**Structure Determination for 2.** A full sphere of low-temperature CCD area-detector diffractometer data was measured ( $T$  ca. 153 K; Bruker AXS instrument,  $\omega$ -scans,  $2\theta_{\max} = 58^\circ$ ; monochromatic Mo K $\alpha$  radiation,  $\lambda = 0.71073$  Å) yielding 42 289 reflections, merging after empirical/multiscan absorption correction (proprietary software) to 5905 unique ( $R_{\text{int}} = 0.082$ ), 4068 with  $F > 4\sigma(F)$  being considered observed and used in the full matrix least squares refinement; anisotropic thermal parameter forms were refined for the non-hydrogen atoms, ( $x, y, z, U_{\text{iso}}^{\text{H}}$ ) constrained at estimates. Difference map residues well removed from the complex were modeled in terms of water molecule oxygen atoms, O(1) fully occupied and O(2–5) occupancies set at 0.5 after trial refinement, associated hydrogen atoms not being located. The complex itself exhibits an interesting disorder, all constituent atoms being modeled in terms of pairs of fragments, site occupancies refining to 0.797(1) and complement, so that each pair has a major and minor component. In the case of the ligand this translates into a pair of components rotationally disordered by approximately a right angle. Conventional residuals on  $|F|$  at convergence were  $R = 0.071$ ,  $R_w = 0.084$  (weights:  $(\sigma^2(F) + 0.0004F^2)^{-1}$ ).

(23) Hall, S. R., du Boulay, D. J., Olthof-Hazekamp, R., Eds. *The Xtal 3.7 System*; The University of Western Australia: Perth, 2000.

Neutral atom complex scattering factors were employed within the Xtal 3.7 program system.<sup>23</sup> Pertinent results are given below and in Figure 2 and Table 1.

**Crystal data:**  $2 \cdot 3\text{H}_2\text{O} \equiv \text{C}_{20}\text{H}_{24}\text{Br}_2\text{N}_6\text{NiO}_3$ ,  $M = 615.0$ ; monoclinic, space group  $P2_1/n$  ( $C_{2h}^6$ , No. 14),  $a = 7.7950(7)$  Å,  $b = 13.571(1)$  Å,  $c = 20.789(2)$  Å,  $\beta = 94.538(2)^\circ$ ,  $V = 2192$  Å<sup>3</sup>,  $D_c$  ( $Z = 4$ ) = 1.851 g cm<sup>-3</sup>,  $\mu_{\text{Mo}} = 46$  cm<sup>-1</sup>; specimen: 0.14 × 0.12 × 0.06 mm;  $T_{\text{min,max}} = 0.58$  0.86.

**Acknowledgment.** Grants from the Australian Research Council and the University of Western Australia (to M.V.B.) and an Australian Postgraduate Research Award (to C.C.W.) are much appreciated. We thank Dr. Anthony Reeder for assistance with mass spectrometry.

**Supporting Information Available:** Full details of crystallographic study of  $2 \cdot 3\text{H}_2\text{O}$ , including tables giving all crystallographic data, atomic positional parameters, bond distances and angles, and anisotropic thermal parameters. This information is available free of charge via the Internet at <http://pubs.acs.org>.

OM011031L